

Partitioned Successive-Cancellation List Flip Decoding of Polar Codes

Charles Pillet*, Ilshat Sagitov*, Grégoire Domer†, and Pascal Giard*

*Department of Electrical Engineering, École de technologie supérieure, Montréal, Québec, Canada.

Email: {charles.pillet.1,ilshat.sagitov.1}@ens.etsmtl.ca, pascal.giard@etsmtl.ca

†Department of Electrical Engineering, Enseirb-Matmeca, Bordeaux INP, Bordeaux, France.

Email: gregoire.domer@enseirb-matmeca.fr

Abstract—The recently proposed Successive-Cancellation List Flip (SCLF) decoding algorithm for polar codes improves the error-correcting performance of state-of-the-art SC List (SCL) decoding. However, it comes at the cost of a higher complexity. In this paper, we propose the Partitioned SCLF (PSCLF) decoding algorithm, an algorithm that divides a word in partitions and applies SCLF decoding to each partition separately. Compared to SCLF, PSCLF allows early termination but is more susceptible to cyclic-redundancy check (CRC) collisions. In order to maximize the coding gain, a new partition design tailored to PSCLF is proposed as well as the possibility to support different CRC lengths. Numerical results show that the proposed PSCLF algorithm has an error-correction performance gain of up to 0.15 dB with respect to SCLF. Moreover, the proposed CRC structure permits to mitigate the error-correction loss at low frame-error rate (FER) due to CRC collisions, showing a gain of 0.2 dB at a FER of 10^{-4} with respect to the regular CRC structure. The average execution time of PSCLF is shown to be 1.5 times lower than that of SCLF, and matches the latency of SCL at $\text{FER} = 4 \cdot 10^{-3}$ and lower.

I. INTRODUCTION

Since the joint invention of polar codes and the asymptotically capacity-achieving Successive-Cancellation (SC) decoding algorithm [1], progress towards improving the error-correcting performance of SC at finite block length has been made by proposing new decoding algorithms of polar codes [2], [3]. SC List (SCL) is the list decoding algorithm based on SC [2]. SCL tracks in parallel a list of L candidates which improves the error-correcting performance. The error-correcting performance of SCL can further be improved by a concatenation of a cyclic-redundancy check (CRC) code with the polar code. This scheme is referred as CRC-aided (CA)-polar codes and has been chosen as one of the coding scheme in the 5G standard [4].

An alternative decoding algorithm of CA-polar codes based on SC decoding is SC Flip (SCF) [3]. While the list of candidates was generated in parallel for SCL, the list of candidates is generated sequentially for SCF by flipping potential error-prone bits after the first SC trial. The accuracy of identifying error-prone bits improved in [5] while also enabling multi-flipping in additional SC trials. SCF and its variants have a variable execution time, but a throughput and a complexity asymptotically equal to those of SC.

Partitioned polar codes [6], [7] are a special type of CA-polar codes. Partitioned polar codes are segmented into parti-

tions, each of which is protected by its own CRC. SCL [6], [7] and SCF [8] support the decoding of partitioned polar codes and are referred to as Partitioned SCL (PSCL) and Partitioned SCF (PSCF). For PSCL, a coding gain with respect to SCL has been observed [6], [7]. Moreover, at equal error-correcting performance, the decoding complexity is reduced [7] as well as the memory requirements if the partitions correspond to sub-decoding trees [6]. For PSCF, the number of flipping trials has been shown to be dividable by a factor 4 with respect to SCF for an equivalent error-correcting performance [8].

Successive-Cancellation List Flip (SCLF) is the flip decoding algorithm based on SCL [9]. If the first SCL fails, a list of path-flipping locations is retrieved and SCL is performed once more and take the L worst paths at the flip location [10], [11]. Various flip metrics have been proposed to find the path-flipping locations. A reliable flipping set based on a heuristic parameter is proposed [12]. Authors in [13] reduce drastically the complexity of this flip metric. A dynamic flipping set permitting to adjust the candidate flip locations was proposed in [14]. SCLF supports multiple flip locations [12], [14] but doing this increases the number of decoding attempts, and thus the decoding complexity. By combining list and flip decoding strategy, SCLF returns the state-of-the-art error-correcting performance at the cost of increased complexity and variable execution time.

In this paper, we propose the Partitioned SCLF (PSCLF) decoding algorithm. We show that it reduces the decoding complexity of SCLF and improves its error-correcting performance. In order to maximise the coding gain with respect to SCLF, the partitions are designed according to the main decoder (SCL). We show that this approach improves error-correcting performance with respect to other partition design strategies [6], [7]. Moreover, a CRC structure is also proposed to reduce CRC false positives, an issue more frequent in PSCLF than in SCLF. The proposed CRC structure improves the error-correcting performance at no additional cost. Finally, the average execution times of PSCLF and SCLF are analyzed and compared to that of SCL and its adaptive variant [15].

II. PRELIMINARIES

A. Polar Codes

A $(N = 2^n, K)$ polar code of length N and dimension K is a binary block code based on the polarization effect

of the binary kernel $\mathbf{T}_2 = \begin{bmatrix} 1 & 0 \\ 1 & 1 \end{bmatrix}$ and of the transformation matrix $\mathbf{T}_N = \mathbf{T}_2^{\otimes n} \in \mathbb{F}_2^{N \times N}$ [1]. A (N, K) polar code is fully defined by its information set $\mathcal{I} \subseteq [N] \triangleq \{0, \dots, N-1\}$, describing the locations where the message $\mathbf{m} \in \mathbb{F}_2^K$ is inserted in the input vector $\mathbf{u} = (u_0, \dots, u_{N-1}) \in \mathbb{F}_2^N$, i.e., $\mathbf{u}_{\mathcal{I}} = \mathbf{m}$. The remaining $N-K$ locations, stored in the frozen set $\mathcal{F} = [N] \setminus \mathcal{I}$ are set to 0, i.e., $\mathbf{u}_{\mathcal{F}} = \mathbf{0}$. The encoding is performed as $\mathbf{x} = \mathbf{u} \cdot \mathbf{G}_N$, where $\mathbf{x} \in \mathbb{F}_2^N$ is a codeword.

A $(N, K+C)$ CA-polar code is a (N, K) polar code concatenated with a CRC code of C bits. The CRC encoder is applied on \mathbf{m} and C CRC bits are appended to \mathbf{m} , defining $\mathbf{m}' \in \mathbb{F}_2^{K+C}$. Hence, \mathcal{I} is now enlarged by C additional bits. As a rule, we have $\mathcal{I} = \{i_1, i_2, \dots, i_{K+C}\}$ with $i_1 < i_2 < \dots < i_{K+C}$. In the remaining of the paper, CA-polar codes are used and decoded with SC-based [1] algorithms. SC leads to poor error-correcting performance in the finite-length regime but can be improved with more complex SC-based decoding algorithm.

B. SCL Decoding

SCL is the list decoding algorithm also based on SC [2]. Hence the scheduling is as SC and at each information bit $i \in \mathcal{I}$, the paths consider both possible values $\{0, 1\}$, doubling the size of the list. In order to limit the complexity, SCL only considers L different decoding paths such that path sorting according to a metric is required. If $i \in \{i_1, \dots, i_{\log_2(L)}\}$, no path sorting is needed since doubling the number of candidates still generates less than or exactly L candidate paths. However, if $i \in \{i_{\log_2(L)+1}, \dots, i_{K+C}\} \triangleq \mathcal{I}_{\text{sort}}$, the L paths minimizing the path metrics out of the $2L$ candidate paths are selected [16]. The path metric $\text{PM}_i[l]$ for index $i \in [N]$ and path $l \in [2L]$ is penalized whenever the bit decision $\hat{u}_i[l]$ of the partial candidate vector $\hat{\mathbf{u}}_0^i[l] \in \mathbb{F}_2^{i+1}$ does not correspond to the hard decision of the log-likelihood ratio (LLR) $\lambda_{0,i}[l]$ in the i^{th} leaf of path l . SCL returns L candidates for \mathbf{u} , noted $\hat{\mathbf{u}}[l]$ with $0 \leq l \leq L-1$. The candidate passing the CRC with the lowest path metric is chosen as decoder output $\hat{\mathbf{u}}$ which improves the error-correction performance.

Adaptive-SCL (ASCL) [17] is an iterative decoding algorithm successively increasing the list size L up to a maximum and stops as soon as the CRC code is checked. The complexity of ASCL converges to SC at low frame-error rate (FER), but the time complexity increases and depends from the channel condition.

C. SCF Decoding

SCF decoding performs up to T_{max} SC decoding trials. A CRC check is performed at the end of each trial. If the first trial fails, a set of flipping candidates β is generated with $|\beta| = T_{\text{max}} - 1$. The t^{th} additional trial performs SC except at the flipping location β_t where the reverse decision on \hat{u}_{β_t} is taken. The decoding latency of SCF is $\mathcal{L}_{\text{SCF}} = T_{\text{max}} \times \mathcal{L}_{\text{SC}}$ while its average execution time $\overline{\mathcal{L}}_{\text{SCF}}$ corresponds to

$$\overline{\mathcal{L}}_{\text{SCF}} = \bar{t} \times \mathcal{L}_{\text{SC}} \leq \mathcal{L}_{\text{SCF}}, \quad (1)$$

where $\bar{t} \leq T_{\text{max}}$ is the average number of decoding trials.

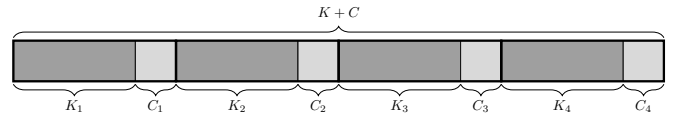


Fig. 1: Message $\mathbf{m}' \in \mathbb{F}_2^{K+C}$ allocated in \mathcal{I} for a partitioned polar code with $P = 4$ partitions. Dark gray corresponds to the message \mathbf{m} and light gray corresponds to the CRC bits.

PSCF [8] is a flip decoder allowing to decode CA-polar codes with multiple CRCs distributed in the codeword. A partitioned polar code is partly described by its set μ corresponding to the last indices of all partitions. The size $P = |\mu|$ describes the number of partitions.

D. SCLF Decoding

SCLF algorithm [9] is the flip decoding algorithm of polar codes with SCL as the core decoder. The best flipping strategy has been proposed in [10], [11]. On a flip location $i \in \mathcal{I}_{\text{sort}}$, the L worst paths are selected instead of the best L paths [2].

If we note the flip metric FM_i^α at index $i \in \mathcal{I}_{\text{sort}}$ and normalized with $\alpha \geq 1$, a factor mitigating the impact of propagation of errors. A reliable flip metric was proposed in [12], later simplified for hardware purpose in [13] as

$$\text{FM}_i^\alpha = -\text{PM}_i[0] + \alpha \text{PM}_i[L], \quad (2)$$

where the path metrics are sorted from most to least reliable. Since a lower complexity SCLF variant is targeted, (2) is selected. The flipping set $\mathcal{B}_{\text{flip}} \subset \mathcal{I}_{\text{sort}}$, storing the indices where the flips are performed, is designed such that $\mathcal{B}_{\text{flip}}(t)$ is the index $i \in \mathcal{I}_{\text{sort}}$ with the t^{th} lowest flip metric [12].

III. PARTITIONED SCLF DECODER

Both SCL and SCF have been adapted to decode partitioned polar codes. The PSCL and PSCF algorithms were shown to have an improved error-correction performance and a reduced decoding complexity over their respective counterparts. SCLF is a more complex algorithm than SCF or SCL, hence we propose the PSCLF algorithm and study the complexity reduction.

A. Partitioned Polar Codes

A partitioned polar code is divided into $P > 1$ partitions. Each partition should contain $K_p \geq 1$ information bits and is concatenated with its own CRC code of size C_p . The number of information bits and CRC bits verify $K = \sum_{p=1}^P K_p$ and $C = \sum_{p=1}^P C_p$. Thus, the partitioned polar code is as well defined with $|\mathcal{F}| = N - K - C$ and $|\mathcal{I}| = K + C$. Fig. 1 depicts the message $\mathbf{m}' \in \mathbb{F}_2^{K+C}$ for $P = 4$ partitions. The vector \mathbf{m}' is then allocated in the positions stated in \mathcal{I} , retrieving \mathbf{u} and the polar encoding is performed to retrieve the codeword \mathbf{x} .

In the following, the number of non-frozen bits in the p^{th} partition is noted $s_p = K_p + C_p$ while the cumulative number of non-frozen bits is noted $S_p = \sum_{i=1}^p s_p$ where $S_1 \triangleq s_1$ and $S_P \triangleq K + C$. Inside a codeword, the last indices of each partition are stored in $\mu = \{\mu_1, \dots, \mu_{P-1}\}$ and $\mu_p \triangleq \mathcal{I}(S_p) = i_{S_p}$.

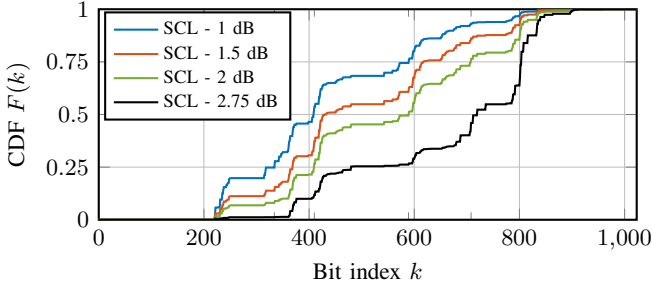


Fig. 2: CDF $F(k)$ of $(1024, 512 + 32)$ polar code for $L = 4$ and $\frac{E_b}{N_0} = \{1, 1.5, 2, 2.75\}$ dB.

A elementary design of partitions μ is to uniformly distribute the partitions based on the information set \mathcal{I} [7]. Namely, it corresponds to the case where $s_p = K_p + C_p = \frac{K+C}{P}$ for any p . Such design of μ will be denoted μ_{eq} . For a code $(1024, 512 + 32)$ and $P = 4$, each partition contains $\frac{K+C}{P} = 136$ non-frozen bits. Another simple design of the partition μ is to consider partitions as sub-decoding trees [6]. For P partitions, each partition is of length $\frac{N}{P}$. However, this approach may lead to partitions without information bits for low-rate codes. Therefore, this approach is not considered.

B. Partition Design Based on SCL

In this paper, partitioned polar codes are decoded with PSCLF, a flip decoder based on SCL. Hence, we propose to design the partitions, i.e., the set μ according to the decoding behaviour of SCL. Next, we denote by X the random variable describing the first error in SCL for a polar code defined by \mathcal{I} . The first error in SCL corresponds to the first index $i \in [N]$ where $\forall l \in [0, L-1], \hat{\mathbf{u}}_0^i[l] \neq \mathbf{u}_0^i$, i.e., all paths have diverged. If $i \in \mathcal{F}$, no paths duplication is performed such that the first error cannot occur. It cannot also occur when all decoding paths are covered, namely if $i \in \{i_1, \dots, i_{\log_2(L)}\}$. Hence, the events of X are only possible in $\{i_{\log_2(L)+1}, \dots, i_{K+C}\} \triangleq \mathcal{I}_{\text{sort}}$. The Cumulative Density Function (CDF) of X is denoted $F(k)$, and is defined as

$$F(k) = \mathbb{P}(X \leq k) = \sum_{i=0}^k \mathbb{P}(X = i), \quad (3)$$

where $\mathbb{P}(X = i) = 0$ if $i \in \mathcal{F}$ or $i \in \{i_1, \dots, i_{\log_2(L)}\}$.

Fig. 2 depicts $F(k)$ for $L = 4$ of a $(1024, 512 + 32)$ polar code at $\frac{E_b}{N_0} = \{1, 1.5, 2, 2.75\}$ dB. As seen in Fig. 2, the probability that the first error occurs earlier in $\hat{\mathbf{u}}$ increases with the noise. For instance, the location delimiting half of the first errors, i.e., $F(k) = 0.5$ is reached at $k = \{409, 433, 590, 720\}$ for $\frac{E_b}{N_0} = \{1, 1.5, 2, 2.75\}$ dB, respectively.

Fig. 3 depicts $F(k)$ of a $(1024, 512 + 32)$ polar code for various list sizes L , all at a $\frac{E_b}{N_0} = 2$ dB. As seen in Fig. 3, as the list size L grows, the probability to have a first error early in the frame decreases. It is explained by the shift to the end of the first index of $\mathcal{I}_{\text{sort}}$ and the improved error capability of SCL with a larger list size. The location delimiting a

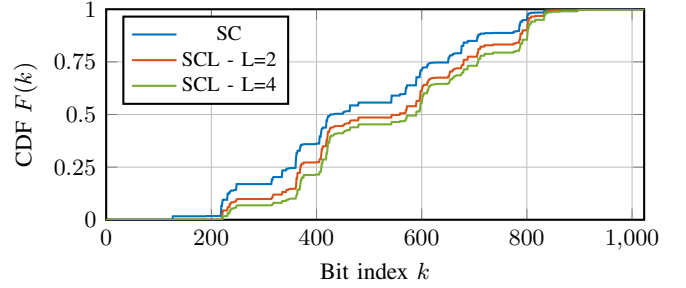


Fig. 3: CDF $F(k)$ of $(1024, 512 + 32)$ polar code for various list sizes L at $\frac{E_b}{N_0} = 2$ dB.

quarter of the first errors, i.e., $F(k) = 0.25$ is reached at $k = \{361, 370, 410\}$ for $L = \{1, 2, 4\}$, respectively.

The proposed design of μ is to uniformly distribute the partitions according to the CDF $F(k)$. Namely, $\forall p \in \{1, \dots, P\}, \mu_p$ verifies

$$F(\mu_p - 1) < \frac{p}{P} \leq F(\mu_p). \quad (4)$$

A similar design for PSCF was carried out by using the decoding behaviour of SC [8]. Since the proposed PSCLF algorithm uses SCL as its core decoder, the CDFs are based on the decoding behaviour of SCL. Given Fig. 2 and for a simulation using SCL with $L = 4$, the two sets μ are

$$\mu = \{335, 409, 589, 1023\}, \quad (5)$$

$$\mu = \{410, 590, 708, 1023\}, \quad (6)$$

for a design at 1 and 2 dB. The number of non-frozen bits in each partition is based on μ and the information set \mathcal{I} of the polar code. For these particular examples, the number of non-frozen bits $\mathcal{K} = \{s_1, s_2, s_3, s_4\}$ inside each partition is $\mathcal{K} = \{28, 32, 100, 384\}$ if μ (5) and $\mathcal{K} = \{61, 100, 84, 299\}$ if μ (6). All partitions are protected by a CRC code and given the sets \mathcal{K} , the number of non-frozen bits fluctuates heavily with the partitions. For both μ , s_1 is small while s_P is large. Next, we discuss the CRC structure of partitioned polar codes.

C. CRC Structure of the Partitioned Polar Codes

With the exception of [18], partitioned decoding of polar codes is usually carried out with a fixed number of CRC bits per partitions. Defining the set of CRC-code size per partition as $\mathcal{C} = \{C_1, \dots, C_P\}$, most works have $C_1 = \dots = C_P$. In [18], the CRC structure was designed according to the capacity of the sub-channels given a set μ . As a consequence, this method designs the CRC structure according to the length of the partitions as well as the reliability of the polar code. However, the design of μ was not discussed and $\mu = \{255, 511, 767, 1023\}$ was chosen with $\mathcal{K} = \{20, 123, 156, 245\}$ non-frozen bits in each partition. The resulting CRC structure is $\mathcal{C}_1 = \{3, 11, 10, 8\}$ [18].

Our proposed CRC structure \mathcal{C} is designed according to the probability of error in each partition and the decoding behaviour of SCL. In a partition, an error is either caused by

	Partition p			
	1	2	3	4
1	0.53	0.23	0.17	0.07
1.5	0.37	0.25	0.24	0.14
2	0.25	0.25	0.25	0.25
2.75	0.09	0.14	0.21	0.56
E_b/N_0 dB	Probability $\mathbb{P}(e_p)$ that the first error occurs in partition p .			

TABLE I: Probabilities that the first error occurs in each partition, the set μ is designed at 2 dB (6).

having no paths passing the CRC or having one path passing the CRC but being a false positive, i.e., a CRC collision. The former may end up getting corrected by a decoding-path flip. The latter, however, cannot be corrected by PSCLF since only wrong paths will end up being forwarded to the next partition. Hence, CRC collisions should be reduced and the proposed CRC structure does so by taking the probability of errors in each partition into account.

Given Fig. 2, at low $\frac{E_b}{N_0}$ values, a decoding error is mostly due to an error happening in the earlier indices of a codeword while at high $\frac{E_b}{N_0}$ values a decoding error is mostly occurring in the latter indices. Table I shows the probability that the first error occurs for each partition, the set μ is designed at 2 dB (6). For a given partition p and $\frac{E_b}{N_0}$, the probability $\mathbb{P}(e_p)$ that the first error occurs can be retrieved from Fig. 2, i.e.,

$$\mathbb{P}(e_p) = F(\mu_p) - F(\mu_{p-1} + 1). \quad (7)$$

The number of CRC bits are allocated according to the target signal-to-noise ratio (SNR). If the design is performed at $\frac{E_b}{N_0} = 1$ dB, more CRC bits should be allocated in the first partition since $P(e_1) = 53\%$. If the design is performed $\frac{E_b}{N_0} = 2.75$ dB, more CRC bits should be allocated towards the last partition since $p(e_4) = 56\%$.

D. Description of PSCLF Decoding

PSCLF decoding requires knowledge of \mathcal{C} and μ . On each partition, up to T_{\max} SCL trials are performed. After reaching μ_1 for the first time, the flipping set β is computed only when none of the paths satisfy the CRC code. If T_{\max} trials are performed and still no paths satisfy the CRC, decoding failure is raised. If at a trial $1 \leq t \leq T_{\max}$, the CRC is checked for at least one path, the decoding of the next partition begins.

For the sake of simplicity, the *check and keep* method, as described in [19], is used when the SCL decoder faces CRC bits inside a codeword. In this method, when performing a CRC check, both paths that satisfy the CRC and those that do not are kept and forwarded to the next partition. This method corresponds to the original SCL algorithm since no changes are made to the algorithm, however, it suffers from a small performance degradation compared to other methods requiring more data control [19].

Decoding is successful if all P CRC codes corresponding to each partitions are satisfied. PSCLF naturally implements *early termination* as decoding stops before the end of a frame whenever a decoding failure happens at a partition $1 \leq p < P$.

E. Average Execution Time of PSCLF

In [8], the complexity of PSCF was linked to the *normalized average computational complexity*. However, no equations were given to compute it. In the following, we provide detailed equations to compute the average execution time of both PSCF and PSCLF. Since the partitions are of different lengths, the impact of flipping fluctuates from partition to partition. The partial latency $\mathcal{L}_{\text{SC}}(i)$ required by the semi-parallel SC decoder to decode until the bit $i \in [N]$ is derived from [20]

$$\mathcal{L}_{\text{SC}}(i) = \sum_{s=0}^{n-1} \left\lceil \frac{2^s}{\varphi} \right\rceil + \sum_{s=0}^{n-1} \left(\left\lceil \frac{2^s}{\varphi} \right\rceil \times \left\lfloor \frac{i}{2^s} \right\rfloor \right), \quad (8)$$

where φ is the number of processing elements. If $i = N - 1$ and corresponds to the end of the decoding, the latency of SC is retrieved, i.e., $\mathcal{L}_{\text{SC}} = \left(2N + \frac{N}{\varphi} \cdot \log_2 \left(\frac{N}{4\varphi} \right) \right)$ [21].

The latency of SCL is given in [22] as $\mathcal{L}_{\text{SCL}} = \mathcal{L}_{\text{SCL}}(N - 1) = \mathcal{L}_{\text{SC}} + |\mathcal{I}|$. Similarly to SCF's (1), the average execution time of SCLF is $\overline{\mathcal{L}_{\text{SCLF}}} = \mathcal{L}_{\text{SCL}} \times \bar{t}$ where \bar{t} is the average number of SCL trials per frame. The partial SCL latency $\mathcal{L}_{\text{SCL}}(i)$ depends on the number of sorting operations required up to index i . Given that $\mathcal{K} = \{s_1, \dots, s_P\}$ is the set storing the number of non-frozen bits in each partition, the SCL partial latency $\mathcal{L}_{\text{SCL}}(\mu_p)$ to decode the first p partitions is

$$\mathcal{L}_{\text{SCL}}(\mu_p) = \sum_{m=1}^p s_m + \mathcal{L}_{\text{SC}}(\mu_p), \quad (9)$$

where the left term represents the number of sorting operations by the end of the p^{th} partition. To compute the average execution of PSCLF, early-termination has to be taken into account. Next, the probability that decoding is performed in partition p is noted $\mathbb{P}(T_p)$. The probability is linked to early-termination since it corresponds to the probability that decoding has not stopped early in any of the previous $p - 1$ partitions. For the first partition, the probability is $\mathbb{P}(T_1) = 1$. The average execution time of PSCLF corresponds to the summation of the average time spent in each partition mitigated by the probability $\mathbb{P}(T_p)$ of decoding it:

$$\overline{\mathcal{L}_{\text{PSCLF}}} = \sum_{p=1}^P \mathbb{P}(T_p) \bar{t}_p (\mathcal{L}_{\text{SCL}}(\mu_p) - \mathcal{L}_{\text{SCL}}(\mu_{p-1})), \quad (10)$$

where $1 \leq \bar{t}_p \leq T_{\max}$ is the average number of SCL trials to decode the p^{th} partition and by convention $\mathcal{L}_{\text{SCL}}(\mu_0) = 0$.

IV. SIMULATION RESULTS

All simulations are performed over the additive white Gaussian noise (AWGN) channel using the Binary Phase-Shift Keying (BPSK) modulation. First, code parameters used are $N = 1024$, $K = 512$, and $C = 32$. Then, $N = \{512, 2048\}$ and $K = \{256, 1024\}$ are used to confirm the results. The information set is designed at $\frac{E_b}{N_0} = 2$ dB (1dB for $N = 2048$) while $L = 4$ is used. With $P = 1$, performances of SCL-4 (---), SCLF (—◆—), and ASCL-L with $L > 4$ (-□-) are shown for references. The latter will match the performance of our proposed PSCLF algorithm. We set $T_{\max} = 15$ and the approximation function (2) with $\alpha = 1.2$ is used [12], [13].

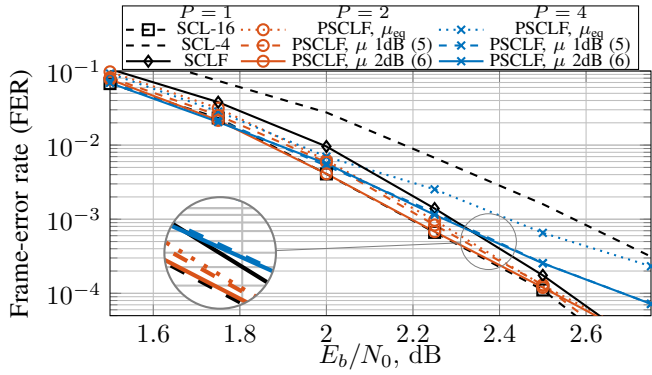


Fig. 4: FER of (1024, 512+32) under SCL, SCLF and PSCLF and various designs of partitions μ .

A. Impact of Partition Designs

Fig. 4 depicts the error-correction performance of PSCLF with various designs of μ . For PSCLF, two uniform structures $\mathcal{C}_{eq} = \{8, 8, 8, 8\}$ for $P = 4$ and $\mathcal{C}_{eq} = \{16, 16\}$ for $P = 2$ are used. The proposed approach based on the CDFs is used to design two partitions μ : $\mu = \{335, \mathbf{409}, 589, \mathbf{1023}\}$ (5), and $\mu = \{410, \mathbf{590}, 708, \mathbf{1023}\}$ (6) that will be compared with the uniformly distributed partitions $\mu_{eq} = \{255, \mathbf{511}, 767, \mathbf{1023}\}$. The boldface values compose the partition for $P = 2$.

For $P = \{2, 4\}$ partitions, the FER is improved by using the proposed designs of partitions μ rather than μ_{eq} . Overall, the FER is better for $P = 2$ than for $P = 4$. Similar observations were made under PSCF [8] or PSCL [6] decoding. For $P = 2$ and $P = 4$, the error-correction performance of PSCLF is better than that of SCLF when using μ (5)–(6) for $\text{FER} \geq 3 \cdot 10^{-5}$ and $\text{FER} \geq 7 \cdot 10^{-4}$, respectively. If μ (5) is used with $P = 2$ ($\text{---}\circ\text{---}$), no loss is observed with respect to SCLF. Up to 0.15 dB gain is observed at $\frac{E_b}{N_0} = 2$ dB if $P = 2$ and μ designed for 2 dB (6) ($\text{---}\circ\text{---}$) which is compliant with our design approach. For $P = 4$, PSCLF suffers from a 0.2 dB loss at $\frac{E_b}{N_0} = 2.75$ dB with respect to SCLF. The crossover happens at $\frac{E_b}{N_0} = 2.3$ dB with μ (5) ($\text{---}\times\text{---}$) and μ (6) ($\text{---}\times\text{---}$) and at $\frac{E_b}{N_0} = 2.1$ dB with μ_{eq} ($\text{---}\times\text{---}$). The error-correction performance is matched with SCL-16.

B. Impact of the CRC Structure

For $P = 4$, simulations with (6) show a performance degradation starting at $\frac{E_b}{N_0} = 2$ dB. As this behavior is not apparent for $P = 2$ with $\mathcal{C} = \{16, 16\}$, this is expected to be an impact of the CRC design. Since the degradation occurs at higher $\frac{E_b}{N_0}$ values, the proposed CRC structure attributes more CRC bits to the last partition. According to Table I, at $\frac{E_b}{N_0} = 2.75$ dB, 56% of the first errors occurs in the last partition. Among these errors, some will cause a collision with a CRC of 8 bits but not with a CRC of 11 bits. Hence, by not passing the enlarged CRC code, flipping is conducted on this partition and the error may get corrected.

Fig. 5 shows an error-correction performance comparison under PSCLF decoding for various CRC structures. The curve

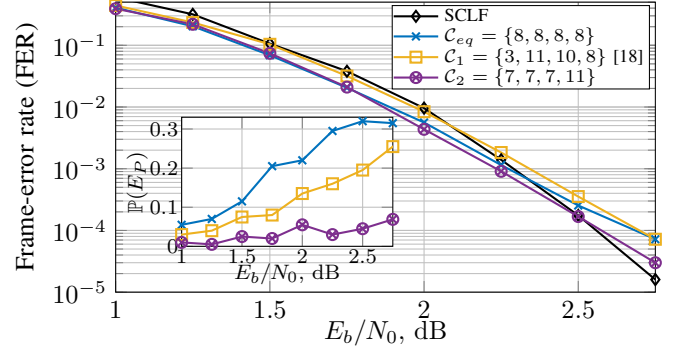


Fig. 5: FER of (1024, 512+32) with multiple CRC structures.

for SCLF decoding is provided as a reference. It can be seen that at a FER of 10^{-4} , using $\mathcal{C}_2 = \{7, 7, 7, 11\}$ ($\text{---}\circ\text{---}$) provides a gain of over 0.15 dB compared to \mathcal{C}_{eq} . From the same figure, it can be seen that the CRC structure $\mathcal{C}_1 = \{3, 11, 10, 8\}$ for a (1024, 512 + 32) polar code from [18] ($\text{---}\square\text{---}$) suffers from error-correction degradation in both low and high SNR. The first partition is protected by only 3 CRC bits, we tracked that there was 3 times more collision occurring in the first partition at low SNR in comparison with the performance by using $\mathcal{C}_2 = \{7, 7, 7, 11\}$. As depicted in Fig. 5, the collision in the last partition also increases with $\mathbb{P}(E_P) = 25.5\%$ for $\frac{E_b}{N_0} = 2.75$ dB. The reason is that the second and third partitions have a small error probability but are protected by a large number of CRC bits, respectively, 11 and 10. This limits the number of CRC bits in the last partition, facing most of the errors.

The probability $\mathbb{P}(E_P)$ that the decoding error is a collision in the last partition is also depicted in Fig. 5. As described previously, by using \mathcal{C}_{eq} , the $\mathbb{P}(E_P)$ increases with $\frac{E_b}{N_0}$ and reaches a $\mathbb{P}(E_P) = 31.5\%$ for $\frac{E_b}{N_0} = 2.75$ dB. Our proposed design reduces the collision $\mathbb{P}(E_P)$ to 6.8% for $\frac{E_b}{N_0} = 2.75$ dB.

C. Partitioned SCLF with $N = 512$ and $N = 2048$

For (2048, 1024 + 32) (respectively (512, 256 + 32)), Figure 6 depicts the error-correction performance of PSCLF with our proposed $\mu = \{819, 1181, 1417, 2047\}$ ($\mu = \{199, 279, 344, 511\}$) and proposed CRC structure $\mathcal{C}_2 = \{7, 7, 7, 11\}$ with respect to $\mu_{eq} = \{511, 1023, 1535, 2047\}$ ($\mu_{eq} = \{127, 255, 383, 511\}$) and $\mathcal{C}_{eq} = \{8, 8, 8, 8\}$. For both codes, using the designed partition μ improves the performance, while the pattern of CRC bits $\mathcal{C}_2 = \{7, 7, 7, 11\}$ improves even more the performance. We observe up to 0.2 dB at $\text{FER} = 10^{-4}$ for $N = 2048$. For both codes, the decoding performance of PSCLF is matched with SCL-16.

D. Average Execution Time of PSCLF

PSCLF improves the decoding performance while reducing the average execution time. This reduction is analysed in this section. All average execution-time curves depicted in Fig. 7 are computed based on Section III-E, by choosing $\varphi = 64$ processing elements in one SC module as selected in [22]. The parallel list implementation is used, i.e., $L = 4$ SC modules are

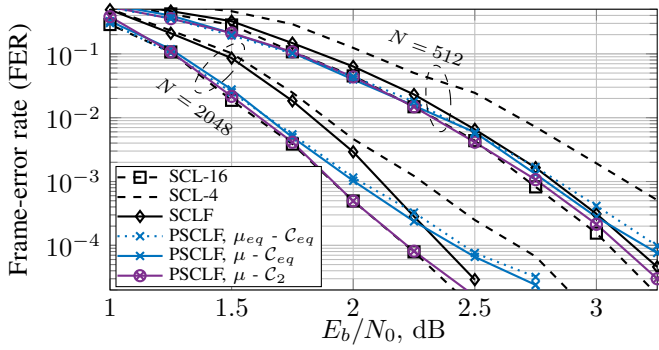


Fig. 6: FER of $(2048, 1024 + 32)$ and $(512, 256 + 32)$ with μ_{eq} and our proposed μ . CRC structures C_{eq} and C_2 are used.

considered for PSCLF. In Fig. 4, ASCL-16 is shown to have similar error-correction performance. For ASCL-16, the use of 4 parallel SC modules is simulated for consistency in terms of area. The average execution time of ASCL and SCLF verify $\overline{\mathcal{L}}_{ASCL} \geq \mathcal{L}_{SC}$ and $\overline{\mathcal{L}}_{SCLF} \geq \mathcal{L}_{SCL}$ with equality if no additional decoding trial is performed. For FER greater than 10^{-3} , the average execution times follow $\overline{\mathcal{L}}_{PSCLF} < \overline{\mathcal{L}}_{ASCL}$.

Fig. 7 depicts $\overline{\mathcal{L}}_{SCLF}$ and the reduction $\overline{\mathcal{L}}_{PSCLF}$ by using our proposed partitioned approach. At FER = 10^{-1} , the reduction is of 29% and 45% for $P = 2$ and $P = 4$, respectively. At FER = 10^{-2} , the reduction is now of 5% and 14% for $P = 2$ and $P = 4$, respectively. The gain is especially visible in undecidable areas where the PSCLF decoding algorithm is early terminating, i.e., does not reach the last partition. By having more partitions, the size of each partition reduces which mitigates the impact of flipping, hence $\overline{\mathcal{L}}_{PSCLF}$ with $P = 4$ is smaller than with $P = 2$. The CRC structure has no impact on $\overline{\mathcal{L}}_{PSCLF}$ such that the proposed CRC structure design should be prioritised over the uniformly distributed CRC structure C_{eq} .

E. Future Research Directions

Reducing the total number of CRC bits C will improve performance for SCLF ($P = 1$). It would be interesting to carry out error-correction and average execution-time comparisons between PSCLF ($P \geq 2$) and SCLF embedding complexity reduction techniques, e.g., a restart mechanism [20].

V. CONCLUSION

In this paper, we proposed the Partitioned SCLF (PSCLF) decoding algorithm. In PSCLF, the code is broken into partitions and each partition is decoded with a CRC-aided SCLF decoder. Numerical results show that the proposed PSCLF algorithm gains up to 0.25 dB with respect to SCLF in terms of FER. To obtain this gain while using a low-complexity flip metric, we proposed a design of partitions and a CRC structure both tailored to PSCLF. The CRC design mitigates the impact of CRC collisions in PSCLF. At a FER of 10^{-4} , the proposed CRC structure was shown to offer a gain of 0.2 dB over the regular CRC structure. The average execution time of PSCLF was estimated to be 1.5 times lower than that of SCLF.

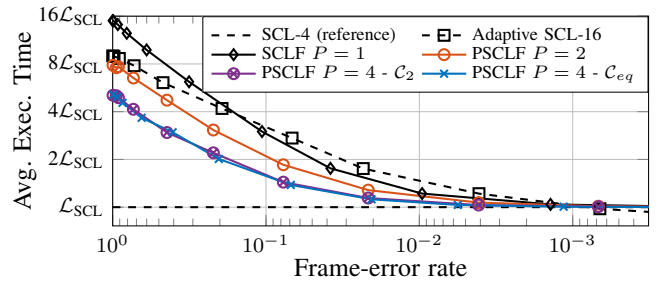


Fig. 7: Average execution time of SCLF, PSCLF, and decoding latency of SCL \mathcal{L}_{SCL} for $(1024, 512 + 32)$ code.

REFERENCES

- [1] E. Arkan, "Channel polarization: a method for constructing capacity-achieving codes for symmetric binary-input memoryless channels," *IEEE Trans. Inf. Theory*, vol. 55, no. 7, pp. 3051–3073, Jul. 2009.
- [2] I. Tal and A. Vardy, "List decoding of polar codes," *IEEE Trans. Inf. Theory*, vol. 61, no. 5, pp. 2213–2226, Mar. 2015.
- [3] O. Afisiadis, A. Balatsoukas-Stimming, and A. Burg, "A low-complexity improved successive cancellation decoder for polar codes," in *Asilomar Conf. on Signals, Syst., and Comput. (ACSSC)*, Nov. 2014.
- [4] 3rd Generation Partnership Project (3GPP), "Multiplexing and channel coding," *3GPP 38.212 V.15.3.0*, 2018.
- [5] L. Chandesaris *et al.*, "Dynamic-SCFlip decoding of polar codes," *IEEE Trans. Commun.*, vol. 66, no. 6, pp. 2333–2345, Jun. 2018.
- [6] S. Hashemi, A. Balatsoukas-Stimming, P. Giard *et al.*, "Partitioned successive-cancellation list decoding of polar codes," in *IEEE Int. Conf. on Acoustics, Speech, and Signal Process. (ICASSP)*, 2016, pp. 957–960.
- [7] H. Zhou, C. Zhang, W. Song *et al.*, "Segmented CRC-aided SC list polar decoding," in *IEEE Veh. Technol. Conf.*, 2016.
- [8] F. Ercan *et al.*, "Partitioned successive-cancellation flip decoding of polar codes," in *IEEE Int. Conf. Commun. (ICC)*, 2018, pp. 1–6.
- [9] Y. Yongrun, P. Zhiwen, L. Nan *et al.*, "Successive cancellation list bit-flip decoder for polar codes," in *Int. Conf. on Wireless Commun. and Signal Process. (WCSP)*, 2018.
- [10] F. Cheng *et al.*, "Bit-flip algorithm for successive cancellation list decoder of polar codes," *IEEE Access*, vol. 7, pp. 58 346–58 352, 2019.
- [11] M. Rowshan and E. Viterbo, "Improved list decoding of polar codes by shifted-pruning," in *IEEE Inf. Theory Workshop (ITW)*, 2019, pp. 1–5.
- [12] Y. Pan, C. Wang, and Y. Ueng, "Generalized SCL-Flip decoding of polar codes," in *IEEE Global Telecommun. Conf. (GLOBECOM)*, 2020.
- [13] F. Ivanov, V. Morishnik, and E. Krouk, "Improved generalized successive cancellation list flip decoder of polar codes with fast decoding of special nodes," *J. of Commun. Netw.*, vol. 23, no. 6, pp. 417–432, 2021.
- [14] Y. Shen *et al.*, "Dynamic SCL decoder with path-flipping for 5G polar codes," *IEEE Wireless Commun. Lett.*, vol. 11, no. 2, pp. 391–395, 2022.
- [15] B. Li *et al.*, "An adaptive successive cancellation list decoder for polar codes with cyclic redundancy check," *IEEE Commun. Lett.*, vol. 16, no. 12, pp. 2044–2047, Nov. 2012.
- [16] A. Balatsoukas-Stimming, M. Parizi, and A. Burg, "LLR-based successive cancellation list decoding of polar codes," *IEEE Trans. Signal Process.*, vol. 63, no. 19, pp. 5165–5179, 2015.
- [17] B. Li, H. Shen, and D. Tse, "An adaptive successive cancellation list decoder for polar codes with cyclic redundancy check," *IEEE Commun. Lett.*, vol. 16, no. 12, pp. 2044–2047, 2012.
- [18] H. Zhou *et al.*, "Segmented successive cancellation list polar decoding with tailored CRC," *J. Signal Process. Syst.*, vol. 91, pp. 923–935, 2018.
- [19] C. Pillet *et al.*, "On list decoding of 5G-NR polar codes," in *IEEE Wireless Commun. and Netw. Conf. (WCNC)*, South Korea, May 2020.
- [20] I. Sagitov, C. Pillet, A. Balatsoukas-Stimming *et al.*, "Generalized restart mechanism for successive-cancellation flip decoding of polar codes," *Under review*, vol. 99, no. 99, pp. 1–12, 9999.
- [21] C. Leroux, A. Raymond, G. Sarkis *et al.*, "A semi-parallel successive-cancellation decoder for polar codes," *IEEE Trans. Signal Process.*, vol. 61, no. 2, pp. 289–299, Jan. 2013.
- [22] P. Giard, A. Balatsoukas-Stimming, T. Müller *et al.*, "PolarBear: A 28-nm FD-SOI ASIC for decoding of polar codes," *IEEE Trans. Emerg. Sel. Topics Circuits Syst.*, vol. 7, no. 4, pp. 616–629, 2017.